Crystal structure, magnetic properties and electronic structure of the MnBi intermetallic compound

2002 J. Phys.: Condens. Matter 14 6509

(http://iopscience.iop.org/0953-8984/14/25/318)

INSTITUTE OF PHYSICS PUBLISHING JOURNAL OF PHYSICS: CONDENSED MATTER

J. Phys.: Condens. Matter **14** (2002) 6509–6519 PII: S0953-8984(02)34054-2

Crystal structure, magnetic properties and electronic structure of the MnBi intermetallic compound

J B Yang[1], W B Yelon[1], W J James[1], Q Cai[2], M Kornecki[2], S Roy[3], N Ali[3] and Ph l'Heritier[4]

[1] Graduate Center for Materials Research and Departments of Chemistry and Physics, University of Missouri—Rolla, Rolla, MO 65409, USA
[2] Department of Physics, University of Missouri—Columbia, Columbia, MO 65211, USA
[3] Department of Physics, Southern Illinois University, Carbondale, IL 62901, USA
[4] ENSPG, Laboratorie des Materiaux et du Genie Physique, UMR 5628 CNRS, 38402 Saint-Martin-D'Heres Cedex, France

Received 20 February 2002, in final form 25 April 2002
Published 14 June 2002
Online at stacks.iop.org/JPhysCM/14/6509

Abstract

The low-temperature phase of the MnBi alloy has a coercivity $\mu_0 H_c$ of 2.0 T at 400 K and exhibits a positive temperature coefficient from 0 to 400 K. In the higher temperature range it shows a much higher coercivity than that of the NdFeB magnets, which suggests that it has considerable potential as a permanent magnet for use at high temperatures. In the temperature range from 30 to 150 K, the Mn atom is found to change its spin direction from a perpendicular to a parallel orientation with respect to the c axis. The anisotropy field increases with increasing temperature which gives rise to a higher coercivity at the higher temperatures. The maximum energy product $(BH)_{max}$ of the magnet is 7.7 and 4.6 MG Oe at room temperature and 400 K, respectively. The electronic structure of MnBi indicates that the Mn atom possesses a magnetic moment of 3.6 μ_B, and that the Bi atom has a magnetic moment of -0.15 μ_B which is due to the s–d and p–d hybridization between Bi and Mn atoms. We have also investigated the volume dependence of the magnetic moments of Mn and Bi. The results indicate that an increase in the intra-atomic exchange splitting due to the cell volume expansion leads to a large magnetic moment for the Mn atom. The Mn magnetic moment attains a value of 4.6 μ_B at a volume expansion rate of $\Delta V/V \approx 100\%$.

1. Introduction

The binary compound MnBi crystallizes into two phases: the lower-temperature phase (LTP) and the high-temperature phase (HTP). The magnetic properties of these MnBi compounds have been studied extensively due to the large uniaxial magnetic anisotropy (2.2×10^7 erg cm^{-3} at 500 K) of the LTP [1, 2] and the magneto-optical properties of the quenched high-temperature

phase (QHTP) [3]. In contrast to most ferromagnetic materials, the coercivity of the LTP increases with temperature, and is much larger than that of the Nd–Fe–B magnets at higher temperatures. Therefore, MnBi has considerable potential as a permanent magnet at high temperatures [4]. However, it is difficult to obtain single-phase MnBi materials by conventional methods, such as sintering. Mn tends to segregate from the MnBi liquid because of the peritectic reaction, and the diffusion of Mn through MnBi is exceedingly slow [5–7]. Many efforts have been made to produce single-phase MnBi [5–16]. At present, no single-phase MnBi has been prepared by sintering Mn and Bi powders [5–12]. LTP MnBi can be prepared by rapid quenching at a speed of about 50 m s^{-1} and subsequent heat treatments [15]. Yoshida *et al* [16] have reported obtaining MnBi of about 90 wt% single phase by zone-arc-melting under a He atmosphere. Roberts and Heiks [6, 8] have reported magnetic moments of 4.0 and 3.95 μ_B/Mn in the LTP obtained by extrapolation to 0 K. A magnetocrystalline anisotropy of 9.0 T and a coercivity of 1.8 T have been measured at 550 K for the melt-spun ribbons, which is very interesting for high-temperature applications [4]. Adams *et al* [9] have produced a MnBi magnet with a maximum energy product of 4.3 MG Oe which is much smaller than the theoretical value of 16 MG Oe. Apart from the technological viewpoint, the magnetic and magnetic–optical properties of MnBi are also most interesting from a fundamental point of view. Theoretical efforts also have been made to explain the magnetic and magneto-optical properties of MnBi [17–21]. Self-consistent spin-polarized band structure calculations for MnBi have been performed by Coehoorn *et al* [17] and the effect of the spin–orbital interaction on the electronic structure has been studied by Jaswal *et al* [20, 21]. However, the theoretical results for the unusual magnetic anisotropy are still in disagreement with the experimental results [14].

In this paper, we report that over 90 wt% LTP MnBi bulk samples can be produced by sintering and subsequent magnetic purification. The dependence of the coercivity and anisotropy on the temperature has been studied using these relatively high-purity materials. A coercivity of 2.0 T and a maximum energy product $(BH)_{max}$ of 4.6 MG Oe have been obtained for MnBi bonded magnets at 400 K. The magnetic structure of MnBi has been investigated by a combination of neutron diffraction techniques and magnetic measurements. Based on the structural information, we have carried out self-consistent band calculations for the LTP MnBi. The volume dependences of the magnetic moments are given, and compared with neutron diffraction refinement data.

2. Experimental and computational methods

We have used different methods to produce the MnBi alloys.

(a) *Sintered method.* High-purity manganese (99.9%) and bismuth (99.99%) were mixed in atomic ratios of 40:60, 45:55 and 50:50. These mixtures were moulded into a columnar shape under a pressure of 4000 kg cm^{-2} and then sintered in an argon atmosphere for 1–10 h at 1000 °C followed by cooling to room temperature. The optimum composition is Mn:Bi = 55:45, where up to 60 wt% of LTP MnBi can be obtained after sintering.

(b) *Mechanical alloying.* The mixed powders were mechanically alloyed, and subsequently annealed at 800 °C for 2 h.

(c) *Induction melting.* The ingots were prepared by induction melting appropriate amounts of Mn (99.99%) and Bi (99.99%) under an argon atmosphere. In order to get a higher purity, magnetic separation was employed in all three methods to enrich the LTP MnBi. The MnBi powders were further ground to fine powders, and aligned in a 10 kOe field in an epoxy resin to form a bonded magnet. Magnetic measurements were performed with a field of up

to 60 kOe in a temperature range from 4.2 to 400 K using a SQUID magnetometer. X-ray diffraction using Cu Kα radiation was employed to determine the presence and extent of the LTP. Neutron powder diffraction data were collected at a wavelength of 1.4807 Å using the diffractometer at the University of Missouri Research Reactor. Neutron diffraction data were analysed using the program FULLPROF, a program for Rietveld analysis of neutron (nuclear and magnetic scattering) or x-ray powder diffraction data [22].

The self-consistent tight-binding-linear-muffin-tin-orbital (TB-LMTO) atomic-sphere-approximation (ASA) method was employed to perform a scalar relativistic band calculation. This method has been described in detail elsewhere [23, 24]. In our calculations, the exchange and correlation term takes the form deduced by von Barth and Hedin [25]. The s, p and d orbitals are used for Mn, and the s, p, d, f orbitals are used for the Bi atoms. The atomic sphere radii are chosen using an automatic procedure developed by Krier *et al* [26]. The calculation is performed for 512 k points in the irreducible parts of the Brillouin zone. The atomic positions of MnBi are scaled according to our experimental results. Convergence is assumed when the root-mean-square error of the self-consistent total energy is smaller than 10^{-6} Ryd. The calculations were also performed for MnBi with various unit cell volumes, so that the dependence of the magnetic properties and total energies on the volumes could be determined.

3. Results and discussion

3.1. Structure and magnetic properties

Figure 1 shows x-ray diffraction patterns of MnBi powders taken at room temperature before and after magnetic purification with different preparative methods. It is found that there are about 50, 30 and 20 wt% of LTP MnBi in the parent alloys after preparation by the sintering (figure 1(a)), induction-melting (figure 1(c)) and mechanical alloying (figure 1(e)) methods, respectively. After magnetic separation, the LTP can be enriched to about 90, 60 and 25 wt% for these methods (figures 1(b), (d) and (f)), respectively. It is apparent that the sintering method is more suitable for producing high-purity LTP MnBi, which is probably due to the good reactivity between Mn and Bi, and to the larger grain size which facilitates the magnetic separation. It can be seen in figure 1(b) that the characteristic peaks of Bi dramatically decrease after magnetic separation of the sintered magnetic LTP MnBi from excess Bi. Neutron diffraction was performed at several different temperatures to determine the magnetic structure of the LTP. Figure 2 shows the neutron diffraction pattern of MnBi after magnetic separation at different temperatures. It is found that there is ≈90 wt% of LTP MnBi in the magnetically separated powders. The MnBi alloys have the NiAs-type structure, space group $R\overline{3}m$ with lattice parameters $a = 4.2827$ Å and $c = 6.1103$ Å (see figure 3), which corresponds to the LTP MnBi [8, 14]. The temperature dependence of the angle between the direction of the magnetic moments and the c-axis can be determined very accurately from the neutron data refinements. Figure 4 shows the temperature dependence of the magnetic moments of the Mn atom and the angle between the moments and the c-axis in the MnBi LTP. Manganese possesses magnetic moments of 3.60 μ_B and 4.18 μ_B at room temperature and 10 K, which agrees well with the magnetic measurements on polycrystalline MnBi [4, 6], on single crystals [14], and with theoretical band calculations [18]. We find that below 200 K, the magnetic moments of Mn deviate gradually from the direction parallel to the c-axis and into the direction nearly perpendicular to the c-axis below 50 K. However, the magnetic moment still shows a very small c-axis component at 10 K; i.e., it is not totally in the basal plane. We find that a conic magnetic structure is formed in MnBi from 240 to 10 K. This confirmed the suggestion of

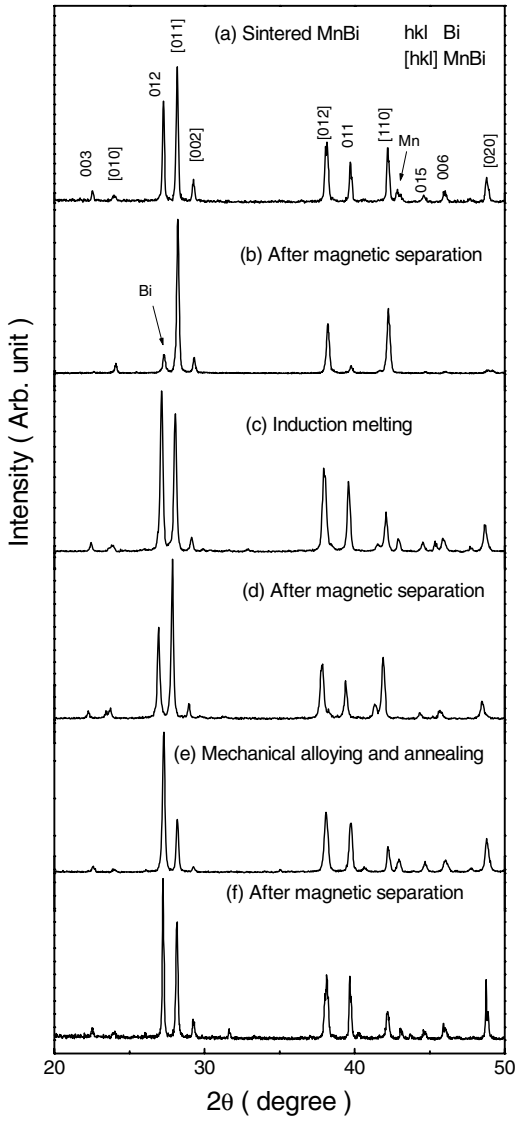

Figure 1. X-ray diffraction patterns of sintered MnBi, before and after magnetic separation.

Roberts [6], that the magnetic moments do not rotate completely from along the *c*-axis into the basal plane at temperatures below 84 K. However, it is different from other studies which concluded that the magnetic moments flip into the basal plane at 90 K [2, 14, 28].

Magnetization curves of MnBi measured perpendicular to the aligned direction are plotted in figure 5. It can be seen that the magnetization curves along the hard axis become easier to saturate when the temperature decreases, which indicates that the uniaxial anisotropy decreases with decreasing temperature, and tends to have planar anisotropy below 100 K. This is consistent with our neutron data. Our neutron data show a conic magnetic structure below 50 K, different from the results obtained from the magnetization curves of an LTP single crystal [14]. Figure 6 shows the temperature dependence of the magnetization of MnBi

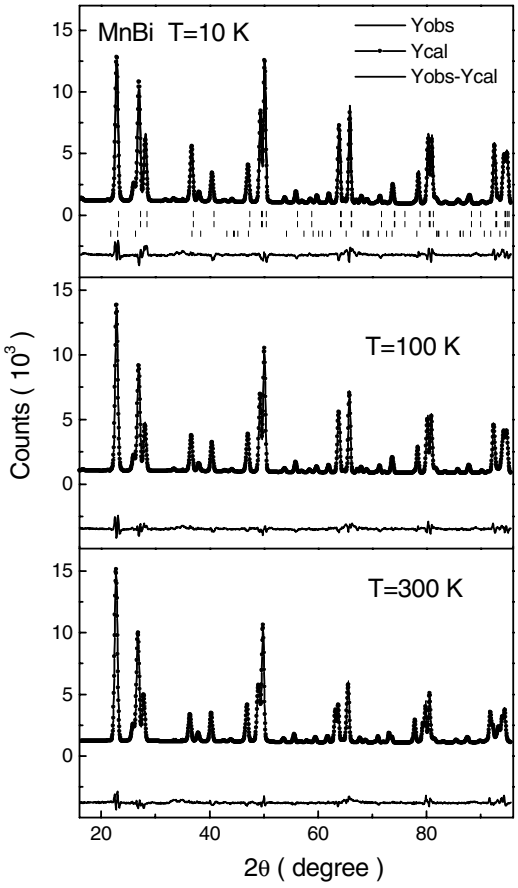

Figure 2. Typical neutron diffraction patterns of MnBi at different temperatures.

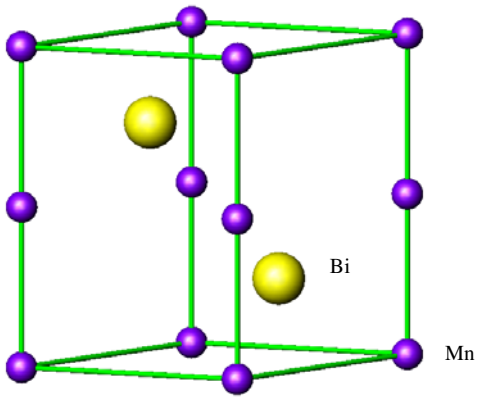

Figure 3. Crystal structure of LTP MnBi.
(This figure is in colour only in the electronic version)

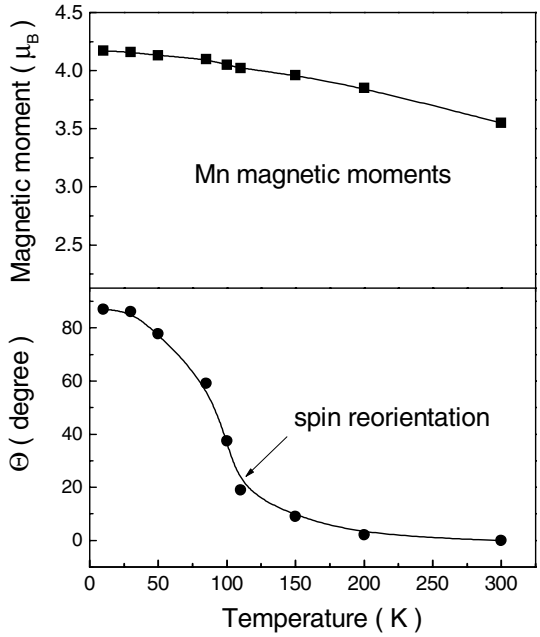

Figure 4. The temperature dependence of the Mn magnetic moments and the angle between magnetic moments and *c*-axis in MnBi.

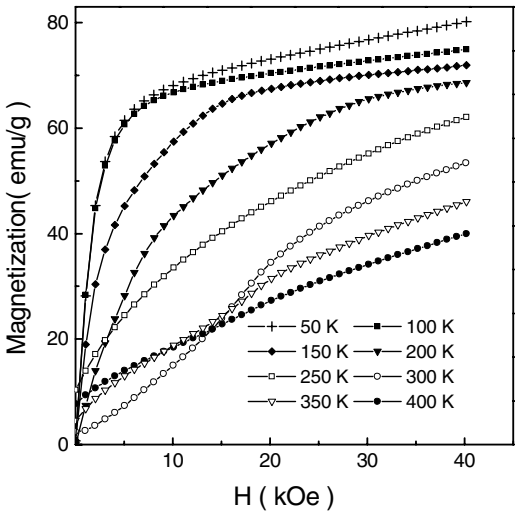

Figure 5. The magnetization curves along the direction perpendicular to the aligned direction at different temperatures.

powders oriented along the *c*-axis at an applied field of 2000 Oe. A sharp maximum related to the spin reorientation is observed at 90 K, which is consistent with the neutron diffraction data. According to our neutron diffraction data and magnetic measurements at different temperatures, the magnetization of Mn is along the *c*-axis from 240 to 650 K. It begins to deviate gradually from the *c*-axis at about 200 K, and continues to approach the *ab*-plane down to 10 K, where the magnetization does not totally lie in the *ab*-plane. Coehoorn *et al* [18] have reported that

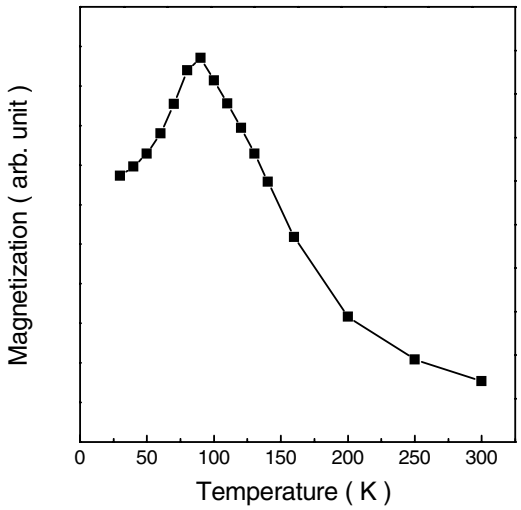

Figure 6. The temperature dependence of magnetization of MnBi along the *c*-axis.

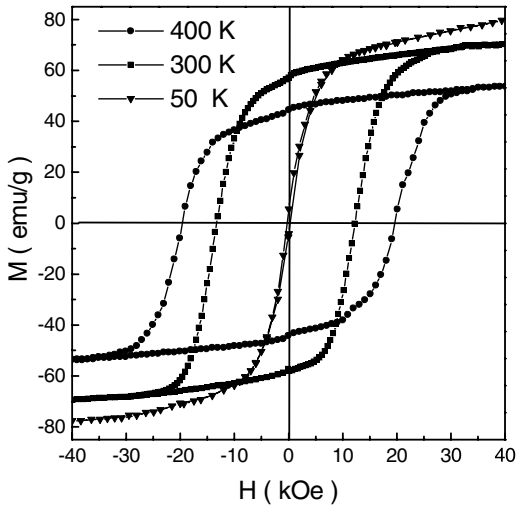

Figure 7. Hysteresis loops of MnBi magnets at different temperatures.

the spin–orbit interaction plays a key role in the anisotropy at low temperatures for MnBi, in as much as the magnetic dipole–dipole interaction cannot explain the basal anisotropy at low temperature. Additionally, recent band calculations with spin–orbital coupling and orbital polarization, still result in disagreement between theoretical and experimental results [21]. Further studies regarding the temperature dependence of the anisotropy of MnBi are necessary.

The MnBi powders are mechanically ground for several hours and the fine powders fixed into an epoxy resin and subjected to a magnetic field of about 1.0 T to form magnetically aligned samples of cylindrical shape. Figure 7 shows hysteresis loops of resin-bonded MnBi magnets measured at different temperatures. Coercivities of 2.0 and 0.004 T have been observed at 400 and 50 K, respectively. As shown in figure 8, the coercivity has a large temperature dependence. The coercivity rapidly increases with temperature from 150 to 400 K; an even

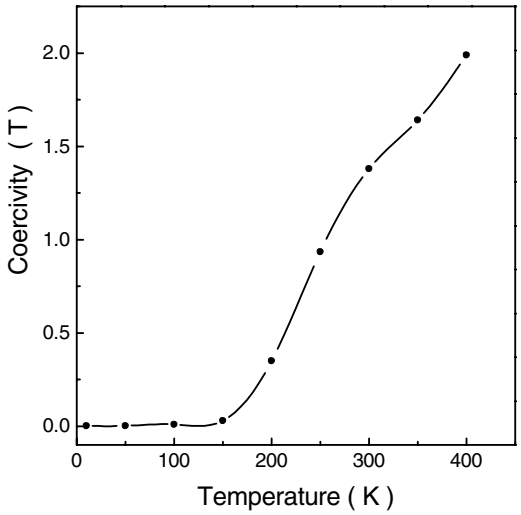

Figure 8. Dependence of the coercivity on temperature for MnBi magnets.

larger coercivity than 2.0 T can be expected at higher temperature. The coercivities in the temperature range 220–300 K are much higher than the values reported for samples prepared by melt-spinning [4], which may be attributed to a different coercivity mechanism. Generally, in melt-spinning where over-quenched ribbons can be obtained, the coercivity field might be mainly controlled by domain wall pinning; however, in our MnBi samples the coercivity is controlled by nucleation hardening. The positive temperature coefficient of coercivity for MnBi magnets above room temperature is a great advantage for high-temperature applications relative to most of the present hard magnets, which have negative coefficients. Below 150 K, the coercivity tends to become zero due to the anisotropy change. The maximum energy product BH_{max} of the magnet is 7.7 MG Oe (61 kJ m^{-3}) and 4.6 MG Oe (37 kJ m^{-3}) at room temperature and 400 K, respectively, which are the largest values reported thus far for MnBi magnets. It is noticed that the relatively low magnetization of MnBi ($M_s = 80$ emu g^{-1}) is a restriction for real application as permanent magnets. Therefore, nanocomposite magnets based on MnBi and a soft phase such as Fe(Co) or Fe_3B might be able to improve the magnetic properties.

3.2. Band structures

Figure 9 shows the density of states (DOS) of each atom in the LTP MnBi. The manganese has a magnetic moment of 3.64 μ_B, whereas Bi has a small induced moment of -0.15 μ_B. These results agree well with those of Coehoorn and de Groot [17]. It should be pointed out that the calculated magnetic moments are smaller than those obtained from neutron diffraction refinements at low temperature, which may be due to the neglect of the orbital contribution to the Mn magnetic moments. There is strong hybridization between the Mn d states and the Bi p states as well as the Bi s and the Mn d states, as can be seen from the identical shape of the partial DOS for Mn and Bi atoms. Because of the hybridization, the calculated magnetic moment of the Mn atom is <4 μ_B, which is a substantial reduction of the free atom moment of 5 μ_B. The partial density of the Mn 3d state is relatively low at the Fermi level, which results in a small electronic specific heat. Our calculated value of $N(E_f)$ is 2.12 states/(eV unit cell) and the electronic specific heat coefficient [29] γ is 2.45 mJ mol^{-1} K^{-2}. Figure 10 shows the

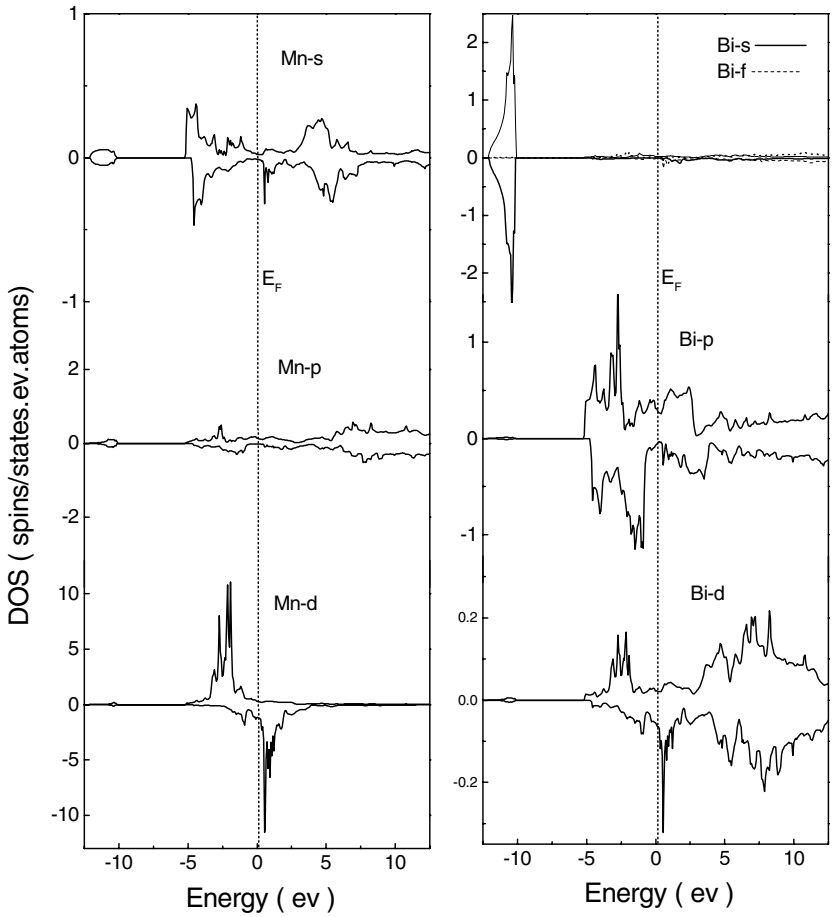

Figure 9. The partial DOS of the each atoms in MnBi.

DOS of LTP MnBi with different unit cell volumes. The volume dependences of the magnetic moments of Mn and Bi are plotted in figure 11. It can be seen from the DOS (figure 10(b)) that the increase of the unit cell volume leads to a narrow bandwidth of the states, and an increase in the intra-atomic exchange splitting, resulting in a large magnetic moment. In the meantime, the overlap between the Mn–Bi atomic states has been reduced. The decreased unit cell volume leads to a broadened bandwidth, and a decrease in the exchange splitting resulting in a lower magnetic moment for the Mn atoms (see figure 10(c)). We have used an antiferromagnetic model for the smaller unit cell volume, but have been unable to achieve a reasonable solution for MnBi. The magnetic moment of Mn increases to a saturated value of 5 μ_B with the increase in unit cell volume which corresponds to a $3d^5$ configuration. The magnetic moment of the Mn atom disappears under a contraction of $\Delta V/V = 75\%$, where no exchange splitting is found for the Mn atomic states. We have also calculated the magnetic moments of the HTP. The Mn atoms appear to have a moment of about 3.5 μ_B, which is much higher than that of the data obtained for the QHTP [14]. The absolute value of the magnetic moment of the Bi atoms increases with expansion of the unit cell, probably due to the high polarization of the large Bi atoms by the Mn magnetic moments.

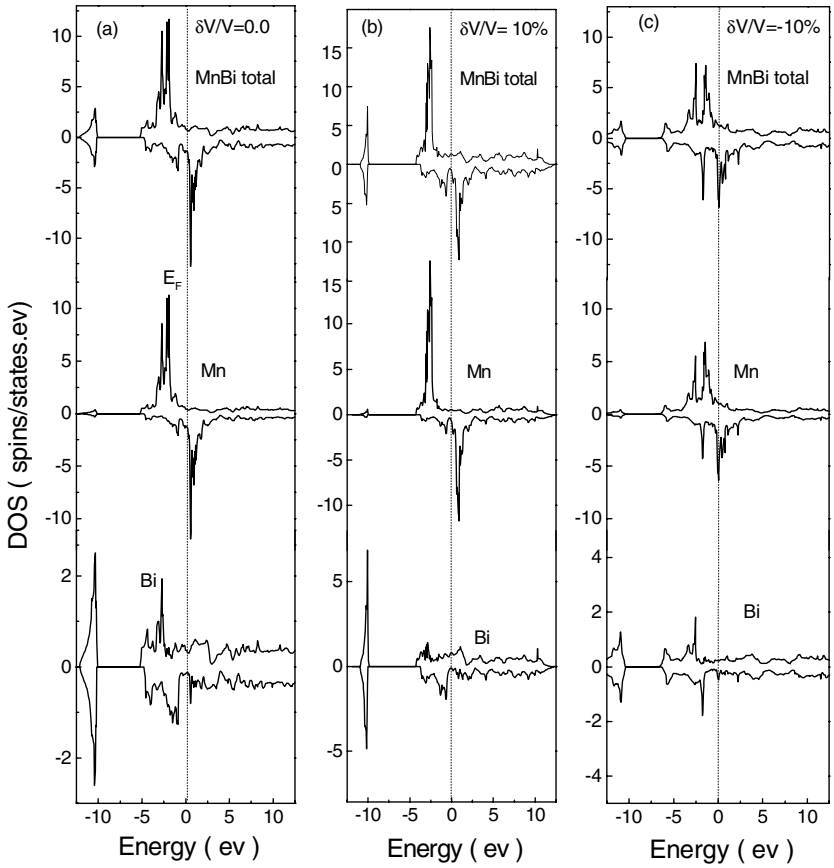

Figure 10. The DOS of MnBi with different unit cell volumes.

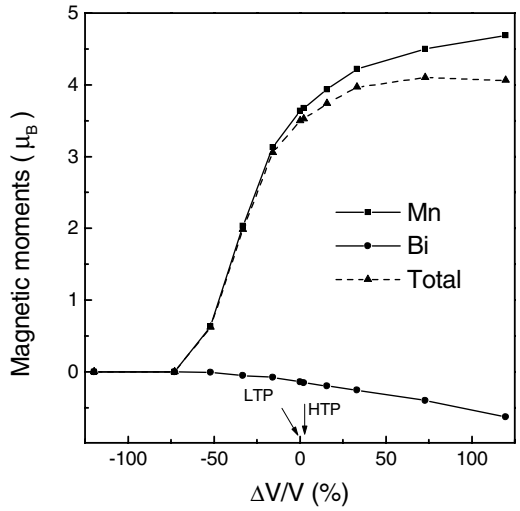

Figure 11. The dependence of the magnetic moment of Mn and Bi atoms on the unit cell volume of the MnBi compound. The arrows marked with LTP and HTP correspond to the unit cell volumes of LTP and HTP of MnBi at room temperature, respectively.

4. Conclusions

Crystal and electronic structures, as well as magnetic properties of the LTP MnBi have been investigated using x-ray diffraction, neutron diffraction, magnetic measurements and band calculations. A spin reorientation of Mn moments has been observed at about 90 K for MnBi. MnBi bonded magnets show a coercivity of 2.0 T at 400 K and exhibit a positive temperature coefficient for coercivity from 0 to 400 K. A maximum energy product of 4.6 MG Oe has been achieved at 400 K. The anisotropy of the MnBi changes from the ab-plane at 0 K to uniaxial anisotropy above 200 K, which leads to the increase of the coercivity. The band calculation reveals that there is strong hybridization between the Mn and the Bi atomic states, which leads to a lower magnetic moment for the Mn atoms. The Mn magnetic moments reach a saturated value of 4.6 μ_B under unit cell volume expansion due to the large exchange splitting.

Acknowledgments

The financial support of the National Science Foundation for grants DMR-9614596 and the Defense Advanced Research Projects Agency for grant DAAG 55-98-1-0267 is acknowledged.

References

[1] Guillaud C 1951 *J. Physique Radium* **12** 143
[2] Stutius W E, Chen T and Sandin T R 1974 *AIP Conf. Proc.* **18** 1222
[3] Chen D and Gondo Y 1964 *J. Appl. Phys.* **35** 1024
[4] Guo X, Chen X, Altounian Z and Ström-Olsen J O 1992 *Phys. Rev.* B **46** 14 578
[5] Andresen A F, Hälg W, Fisher P and Stoll E 1967 *Acta Chem. Scand.* **21** 1543
[6] Roberts B W 1956 *Phys. Rev.* **104** 607
[7] Noothoven van Goor J M and Zijlstra H 1968 *J. Appl. Phys.* **39** 5471
[8] Heikes R R 1955 *Phys. Rev.* **99** 446
[9] Adams E, Hubbard W M and Syeles A M 1952 *J. Appl. Phys.* **23** 1207
[10] Pirich R G 1983 *Met. Trans.* A **11A** 193
Pirich R G 1980 *IEEE Trans. Magn.* **16** 1065
[11] Pirich R G and Larson D J Jr 1979 *J. Appl. Phys.* **50** 2425
[12] Andresen A F, Hälg W, Fisher P and Stoll E 1967 *Acta Chem. Scand.* **21** 1545
[13] Saha S, Huang M Q, Thong C J, Zande B J, Chandhok V K, Simizu S, Obermyer R T and Sankar S G 2000 *J. Appl. Phys.* **87** 6040
[14] Chen T and Stutius W 1974 *IEEE Trans. Magn.* **10** 581
[15] Guo X, Zaluska A, Altounian Z and Ström-Olsen J O 1990 *J. Mater. Res.* **5** 2646
[16] Yoshida H, Shima T, Takahashi T and Fujimori H 1999 *Mater. Trans. JIM* **40** 455
[17] Coehoorn R and de Groot R A 1985 *J. Phys. F: Met. Phys.* **15** 2135
[18] Coehoorn R, Haas C and de Groot R A 1985 *Phys. Rev.* B **31** 1980
[19] Oppeneer P M, Antonov V N, Kraft T, Eschrig H, Yaresko A N and Perlov A Ya 1996 *J. Appl. Phys.* **80** 1099
[20] Jaswal S S, Shen J X, Kirby R D and Sellmyer D J 1994 *J. Appl. Phys.* **75** 6346
[21] Ravindran P, Delin A, James P, Johansson B, Wills J M, Ahuja R and Eriksson O 1999 *Phys. Rev.* B **59** 15 680
[22] Rodriguez-Carvajal J 1995 *Fullprof* version 3.0.0
[23] Andersen O K and Jepsen O 1984 *Phys. Rev. Lett.* **53** 2571
[24] Andersen O K, Pawlowska Z and Jepsen O 1986 *Phys. Rev.* B **34** 5253
[25] von Barth U and Hedin L 1972 *J. Phys. C: Solid State Phys.* **5** 1629
[26] Krier G, Andersen O K and Jepsen O, at press
[27] Lambrecht W R L and Anderson O K 1986 *Phys. Rev.* B **34** 2439
[28] Hihara T and Koi S Y 1970 *J. Phys. Soc. Japan* **29** 343
[29] Kittel C 1976 *Introduction to Solid State Physics* 5th edn (New York: Wiley)